PCCP

Accepted Manuscript

ROYAL SOCIETY OF CHEMISTRY

www.rsc.org/pccp

Journal Name

ARTICLE

Enhanced saturation magnetization in buckypaper-films of thin walled carbon nanostructures filled with Fe_3C, FeCo, FeNi, CoNi, Co and Ni crystals: the key role of Cl

Received 00th January 20xx,
Accepted 00th January 20xx

DOI: 10.1039/x0xx00000x

www.rsc.org/

Jian Guo [a], Mu Lan [a], Shanling Wang [b], Yi He [b], Sijie Zhang [a], Gang Xiang [a **] and Filippo S.Boi [a*]

We report an advanced chemical vapour deposition approach which allows the synthesis of cm-length ultrathin buckypapers comprising carbon nanostructures filled with Fe_3C, FeCo, FeNi, CoNi, Co and Ni directly in situ by sublimation and pyrolysis of single or combined metallocenes with very low quantities of dichlorobenzene. As a result extremely high saturation magnetizations of 117 emu/g, 90 emu/g and 80 emu/g are obtained for the specific case of Fe_3C, FeCo and FeNi, instead variable saturation magnetizations of 70 emu/g, 58 emu/g and 6.7 emu/g are obtained for Co, CoNi and Ni.

A: Introduction

For more than a decade carbon nanotubes (CNTs) filled with ferromagnetic Fe-based crystals like Fe_3C and α-Fe have attracted the attention of numerous researchers owing to their potentially outstanding magnetic properties: high coercivity and high saturation magnetization [1-17]. In particular large coercivities have been achieved by encapsulating small particles with a size in the order of a single magnetic domain inside multiwall CNTs through sublimation and pyrolysis of ferrocene in conventional chemical vapour deposition (CVD) systems [1-8]. However numerous issues have been found in the tunability of the saturation magnetization properties owing to the limited control of the CNTs filling-rates with these conventional methods. Interestingly Boi et al. recently reported two novel methods involving the sublimation and pyrolysis of ferrocene in presence of local perturbations [18] or viscous boundary layers created between a rough surface and the ferrocene/Ar flow [19] that allowed obtaining flower-like and radial multiwall CNTs completely filled with Fe-based crystals. However the presence of an unusual γ-Fe magnetic arrangement in the case of the boundary layer methods, and the unusual oxidation processes observed in the case of the local perturbation method have partially limited the magnetic tunability of these structures.

In this context other CVD methods involving the sublimation of mixtures of metallocenes and Cl-containing hydrocarbons like chlorobenzene, dichlororbenzene and trichlorobenzene have become very attractive for the synthesis of thin-walled CNTs continuously filled with ferromagnetic Fe-based alloy- crystals [20-25]. Indeed the presence of Cl in these mixtures can allow the achievement of extremely high filling rates of the carbon nanotube core (many micrometres). These methods have been mainly used for the fabrication of CNTs- films (buckypapers) filled with Fe-base alloys like Fe_3C [20-22], FeNi [23-25], FeCo [25] and FeCoNi [25]. Furthermore owing to the relatively low coercivity (500 Oe for Fe_3C, 90-450 Oe for FeNi, 350 Oe for FeCo and 750 Oe for FeCoNi), the produced nanostructures can be considered ideal candidates for the production of light-weight bucky-paper electrodes or potentially ideal candidates also for applications as microwave absorber materials where high saturations magnetizations and low coercivities are required. However despite the extremely high filling-rates achieved with these methods, saturation magnetizations much lower than those expected in bulk Fe_3C (169 emu/g), FeCo (220 emu/g) and FeNi (79-168 emu/g) have been reported: 40-45 emu/g for Fe_3C [21], 37-65 emu/g for FeNi [23-25] and 42.5 emu/g for FeCo [25]. The origin of these unusual low saturation magnetizations is still an open problem that limits the translation of these nanostructures in a key technology. Interestingly analysing the literature reports referenced above, different saturation magnetization can be observed depending on the chosen Cl-containing precursor. In the case of FeNi alloys, a decrease in the saturation magnetization from the value of 65 emu/g obtained by CVD of dichlorobenzene/metallocenes (0.05-0.2 g/ml) [23-24], to the lower value of 35-36 emu/g in the case of trichlorobenzene/metallocenes was reported [25]. Furthermore, low saturation magnetizations were observed also in the case of Fe_3C-filled CNTs-buckypapers[21] produced by CVD of trichlorobenzene/ferrocene (0.06 g/ml supplied at the rate of 0.12 ml/min [21]). Previous energy dispersive x-ray (EDX) investigations of the CNT-Fe and -FeNi-filling showed that no trace of Cl could be detected inside the filled-CNTs suggesting that Cl may instead combine with H and etch the CNTs graphitic layers [20,23-24]. The formation of carbon chlorinated clusters which would then enhance the filling rate of the CNTs was also considered [25].

[a] College of Physical Science and Technology Sichuan University, Chengdu China.
[b] Analytical and Testing Centre Sichuan University Chengdu China.
Email first corresponding author: f.boi@scu.edu.cn
Email second corresponding author: gxiang@scu.edu.cn
DOI: 10.1039/x0xx00000x

In this paper we address this open problem by focusing first on the specific case of Fe_3C crystals inside thin walled CNTs comprised in cm-length buckypapers produced by CVD of mixtures of ferrocene and very low quantities of dichlorobenzene (0.05 ml). In the second part of this paper we then focus on the case of thin walled CNTs produced by CVD of mixtures of ferrocene/cobaltocene and ferrocene/nickelocene with dichlorobenzene. In particular, in the attempt to enhance the saturation magnetization of the encapsulated crystals we underline that the quantities of Cl used in our CVD system (0.05 ml) are much lower with respect to those used in the previous literature works [21]. The produced CNTs were characterized through scanning electron microscopy (SEM), backscattered electrons (BE), EDX, transmission electron microscopy (TEM), high resolution TEM (HRTEM), scanning TEM (STEM), and vibrating sample magnetometry (VSM). The VSM measurement show that extremely high saturation magnetizations of 117 emu/g, 90 emu/g and 80 emu/g are obtained in the case of buckypapers comprising CNTs filled with Fe_3C, FeCo and FeNi respectively. Similar ultrathin buckypapers were also synthesized by CVD of nickelocene-cobaltocene, nickelocene and cobaltocene with dichlorobenzene (0.05 ml). Specifically we show that in absence of ferrocene as precursor, the obtained ultrathin buckypapers exhibit a different morphology comprising CNTs partially filled with Ni particles (CVD of nickelocene/dichlorobenzene) and CoNi particles (CVD of nickelocene-cobaltocene/dichlorobenzene) or agglomerates of Co nanoparticles (CVD of cobaltocene/dichlorobenzene) embedded in amorphous carbon. For these specific cases we report a variable saturation magnetization of 6.7 emu/g (Ni), 58 emu/g (CoNi) and 70 emu/g (Co). To the best of our knowledge no works on ultrathin buckypapers have previously reported such high magnetic properties and tunability. Indeed previous works reported the only case of very thin buckypapers comprising CNTs filled with FeNi or Fe_3C with much lower saturation magnetization[21-25]. The extremely high tunability of the magnetic-hysteresis properties make the buckypapers produced with our method ideal candidates for applications in microwave absorption, sensors and many others.

B: Results and Discussion

The synthesis performed by CVD of 30 mg of ferrocene and 0.05 ml of dichlorobenzene revealed the growth of uniform thin-CNTs films on cm-length Si/SiO_2 substrates as the only product in the reactor (see Figs.1A-D). The buckypaper was easily peeled-off from the substrate-surface and attached to carbon-tape films for the SEM analyses. The morphology of the thin walled CNTs comprised in the buckypaper was revealed by SEM micrographs. The typical morphology of the CNTs can be observed in Fig.1A. The thickness of the buckypaper was measured to be of 10-15 micrometers. The high filling rate of the thin walled CNTs was revealed by BE analyses (Fig.1B). In these analyses, due to the atomic number contrast, the CNT-filling appear bright in the image, while the CNTs-walls have a darker-contrast. The high filling rate of the CNTs was also revealed by HRTEM and TEM analyses. In this case a small region of the buckypaper was cut and dissolved in ethanol by sonication. The CNTs were then transferred with a Pasteur pipette in the TEM copper-grid. A typical HRTEM image showing the crystal-lattice spacing corresponding to the 100 reflection of Fe_3C with space group Pnma is shown in Fig.1C. A top view of the analysed continuously-filled CNT is also shown in Fig.1D.

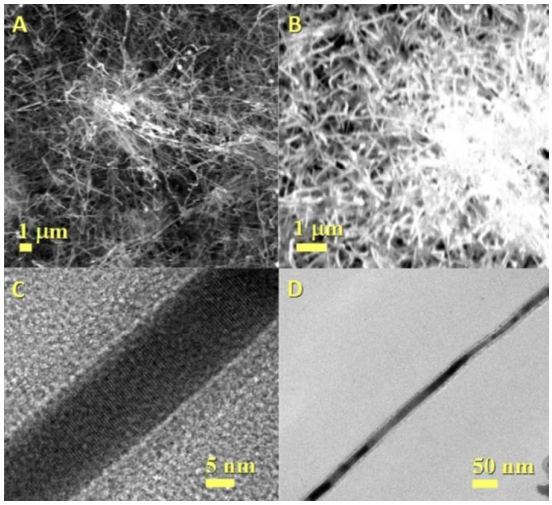

Figure 1: SEM micrograph in A showing the high morphological quality of the CNTs-buckypaper produced from CVD of mixtures of 30 mg of ferrocene and 0.05 ml of dichlorobenzene. In B the BE micrograph shows the high filling rate of the CNTs. In C a typical HRTEM micrograph of a CNT is shown. The observed lattice spacing of 0.5 nm corresponds to the 100 reflection [26] of Fe_3C with space group Pnma. In B the high filling rate of the CNTs is shown from a top view.

Further investigations were then performed with XRD in order to study the structural and phase composition of the buckypaper-film peeled-off from the Si/SiO_2 substrate after CVD of the ferrocene-dichlobenzene mixtures. In particular the presence of a single phase of Fe_3C was revealed in the XRD diffractogram (fitted with Rietveld refinement) of Fig.2 by the (210), (002), (201), (211), (102), (220), (031), (112), (131), (221) and (122) atomic plane-reflections.

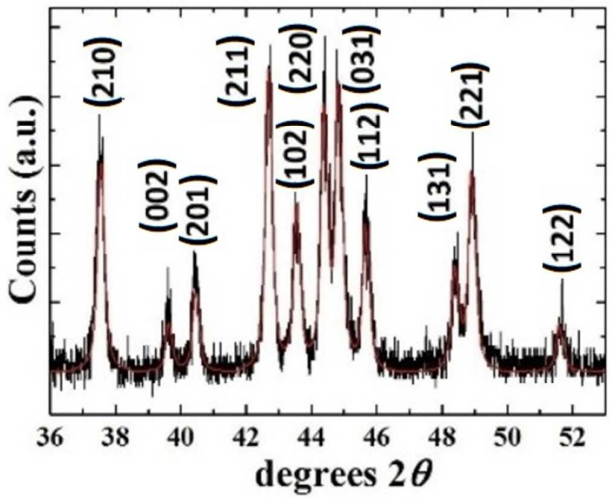

Figure 2: XRD diffractograms (black line) and Rietveld refinement (red line) of a typical buckypaper of CNTs continuously filled with Fe_3C crystals.

The crystallite-grain size was then extracted by using the Scherrer equation[30] and resulted to be 17-20 nm, which is in agreement with the TEM analyses shown in Fig.1.

In order to study the morphological variation of the CNTs-composing the buckypaper with the increase of the ferrocene quantity, further experiments were performed with mixtures of 40 mg of ferrocene and 0.05 ml of dichlorobenzene. Also in this case the CNTs-buckypaper was easily peeled-off from the Si/SiO_2 substrate surface. A small region of the film was then cut and dissolved in ethanol for the TEM sample preparation. Interestingly also in this case the TEM analyses of the CNTs revealed the presence of very high filling rates, however a slightly larger crystal diameter of 10-20 nm was found. The HRTEM image of Fig.3A shows the lattice spacing of 0.5 nm corresponding to the typical 100 reflections of Fe_3C with space group Pnma. In Fig.3B a top view of an area comprising many randomly oriented CNTs is shown. Interestingly in these syntheses conditions other nanostructures were also found as by-product in the quartz tube reactor. The TEM analyses of these by-products revealed the presence of CNTs with a much larger diameter of 0.2-1 micrometres. In particular as shown in Fig. 3C-D also in this case continuous encapsulated crystals were found. However despite the numerous HRTEM measurements, in this specific case no lattice spacings were observed owing to the higher thickness of the crystals encapsulated inside the CNT. In order to investigate the crystallinity and composition of the analysed CNTs-filling, SAED measurements of the encapsulated crystals and EDX analyses in STEM mode were then considered.

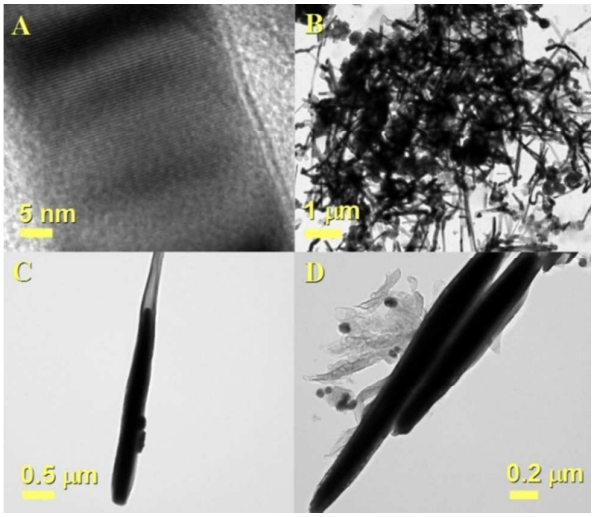

Figure 3: High resolution TEM micrograph showing in A the lattice spacing of 0.5 nm corresponding to the 100 reflection of a Fe_3C single crystal produced from sublimation and pyrolysis of mixtures of 40 mg of ferrocene and 0.05 ml of dichlorobenzene on the top of Si/SiO_2 substrates. In B the high CNTs filling rate is shown from a top view of a large area of the TEM grid. In C and D the CNTs obtained as by-products in the reactor have a much larger diameter with respect to those composing the buckypaper shown in A-B and still a continuous filling.

In Fig.4A-B an example of a CNT-by-product used for the STEM and SAED analyses is shown. In particular the insert shows the STEM image of the filled-CNT. The bright areas represent the crystal filling obtained with the Z-mapping (atomic-number contrast) mode. A typical SAED pattern observed in the areas 1-3 in the inset of Fig.4A

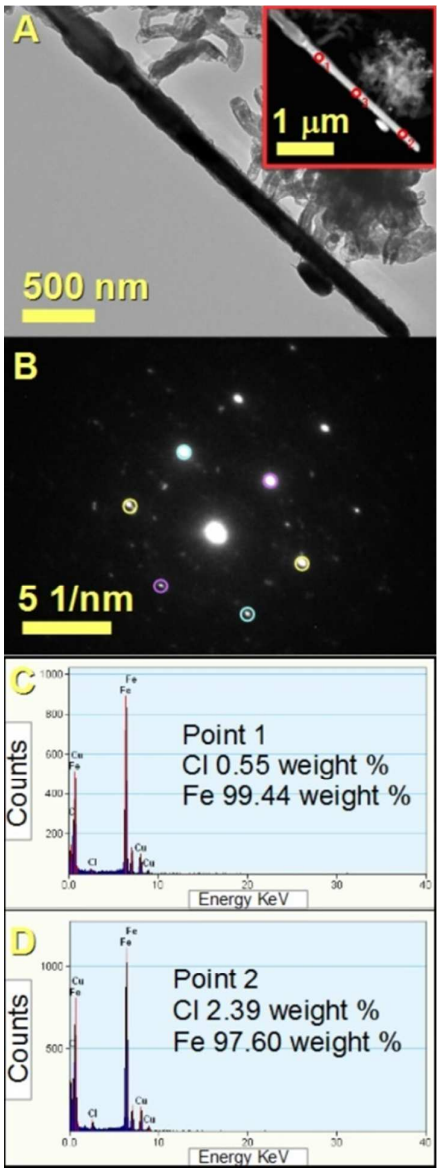

Figure 4: TEM micrograph and STEM-compositional image of the area (inset) showing in A the cross sectional morphological and compositional (bright region observed in Z-contrast mode indicate the CNTs filling) properties of an individual CNT produced from sublimation and pyrolysis of mixtures of 40 mg of ferrocene and 0.05 ml of dichlorobenzene and extracted from the regions of the reactor near the substrate. In B a typical SAED pattern of the region 1 of the CNT filling (see inset in A) showing multiple diffraction spots typical of a mixed single/crystalline-polycrystalline arrangement of Fe_3C. In C and D the variation of the Cl weight % along the CNT-filling shown in the point 1 and 2 of the inset in A is illustrated through STEM -EDX analyses.

can be observed in Fig.4B. Interestingly, together with bright diffraction spots indicating single crystals reflections of the Fe_3C phase (the cyan circles indicate the (220) atomic plane reflection of Fe_3C with space group Pnma corresponding to the lattice spacing of 0.202 nm, the magenta circles indicate the (210) atomic plane reflection of Fe_3C with space group Pnma corresponding to the lattice spacing of 0.236 nm, and the yellow circles indicate the (220) atomic plane reflection of Fe_3C with space group Pnma corresponding to the lattice spacing of 0.198 nm), other small diffraction spots arranged in a circle (same lattice spacing of the spots indicated with magenta circles) corresponding to a polycrystalline crystal arrangement are found. These observations suggest that many crystals can be present inside the CNTs filling in a polycrystalline arrangement. These measurements are very different with respect to those observed in Fig. 1C and Fig.3A where only a single set of lattice spacings typical of a single crystal arrangement with a preferred orientation (with respect to the CNT-axis) was found. Further analyses were then performed with STEM and EDX to investigate the elemental composition of the encapsulated crystal and to check the possible presence of Cl inside the CNTs-filling. Surprisingly the EDX analyses in the point 1 and 2 of the filled-CNT shown in the STEM image of Fig.4A (inset) revealed together with the expected high Fe-content, the presence of variable quantities of Cl inside the encapsulated crystals (the C-content was not considered since the Fe_3C phase, the CNT-walls together with the carbon-film on the TEM copper grid contain C and their contribution can not be isolated). These observations prove that a small variable quantity of Cl can remain trapped in the crystals even if quantities of dichlorobenzene as small as 0.05 ml are used. These observations are very different with respect to those reported in the previous literature works [20-25]. We suggest that the weight % of Cl may be much higher in presence of higher concentration of dichlorobenzene or similar hydrocarbons (i.e. tri-chlorobenzene).

In order to avoid the formation of by-products, further experiments were then performed by using the same small quantities (30 mg) of metallocenes used for the CNTs shown in Fig.1. However in this case the use of cobaltocene (15 mg) and nickelocene (15 mg) together with ferrocene (15 mg) was considered for the synthesis of buckypapers with FeCo and FeNi alloys. Therefore in the case of CNTs-filled with FeCo as first step, 15 mg of ferrocene and 15 mg of cobaltocene were mixed with 0.05 ml of dichlorobenzene and fed into the CVD system. The morphology of the buckypaper grown on the Si/SiO_2 and peeled-off after substrate extraction was revealed by scanning electron micrographs, as shown in Fig.5. A top view of a flake of buckypaper cut for the SEM a analyses and attached to a carbon film-tape is shown in Fig.5A. The thickness of the buckypaper resulted to be 10 micrometres (similarly to that obtained in the case of 30 mg of ferrocene). In B and C, the BE micrographs revealed the continuous filling rate of the CNTs. The diameter of the CNTs in this case was slightly larger with respect to that of the CNTs shown in Fig.1. In particular as shown in Fig.5D a typical CNT analysed by TEM exhibited a diameter of 70-100 nm and a variable encapsulated-crystal diameter in the order of 40-100 nm. The phase and structural composition of the filled CNTs obtained in these conditions was then analysed with XRD. The obtained XRD pattern is shown in Fig.6. Interestingly the presence of a large quantity of FeCo with space group Pm-3m was revealed by the highly intense (110) atomic plane reflection, while small residual peaks of the Fe_3C phase indicate that a minor fraction of the encapsulated crystals (7%) consisted still of Fe_3C. In this specific case the extracted crystallite-grain size was 30.5 nm, suggesting therefore that the produced FeCo alloys possess a multigrain arrangement. These results could also explain the contrast-variation that is frequently observed in the produced CNTs-filling during TEM investigations (see Fig.5D).

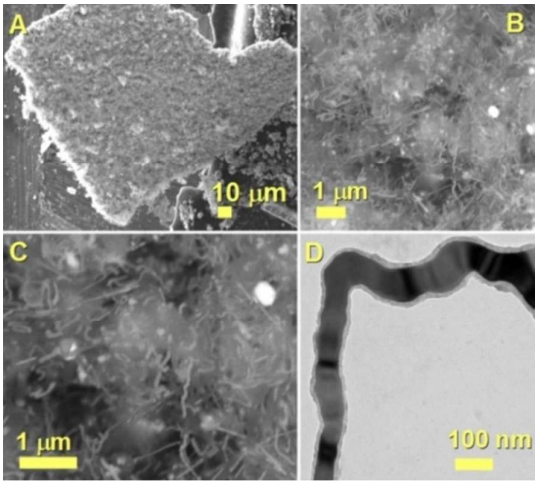

Figure 5: In A a SEM micrograph of a typical buckypaper-flake comprising CNTs filled with FeCo from a top view (A). In B and C two BE micrographs reveal with increasing detail the filling rate of the CNTs. In D a typical TEM micrograph of a thin-walled CNT continuously filled with FeCo is shown. The TEM sample was prepared by first dissolving a small piece of the buckypaper in ethanol. Then (after dissolution through sonication) the CNTs in ethanol were transferred by using a Pasteur pipette in the TEM grid.

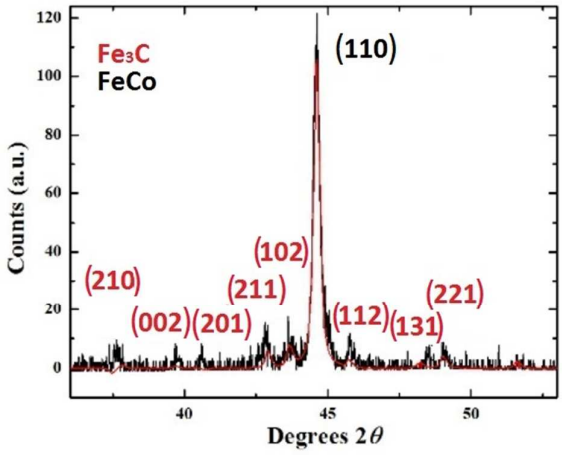

Figure 6: XRD diffractograms (black line) and Rietveld refinement (red line) of a typical buckypaper of CNTs filled with continuous FeCo crystals and minor quantities of Fe_3C crystals.

Similar results were also obtained in the case of buckypapers consisting of CNTs filled with FeNi alloys (see sup.info FigsS1-3 for TEM images, statistical distribution and XRD analyses). In this case the SEM and TEM investigations revealed a crystal diameter in the order of 70-100 nm, while XRD showed the presence of gamma-FeNi in 95% of the sample, with only a residual fraction of Fe_3C (5%) (verified also in this case through Rietveld refinement analyses, see supp. informations Fig.3) and a grain size of 30.5 nm. The investigation of the magnetic properties of the produced buckypapers comprising CNTs continuously filled with Fe_3C, FeCo and FeNi was then considered. The result of the magnetic measurements performed with VSM can be observed in Fig.7.

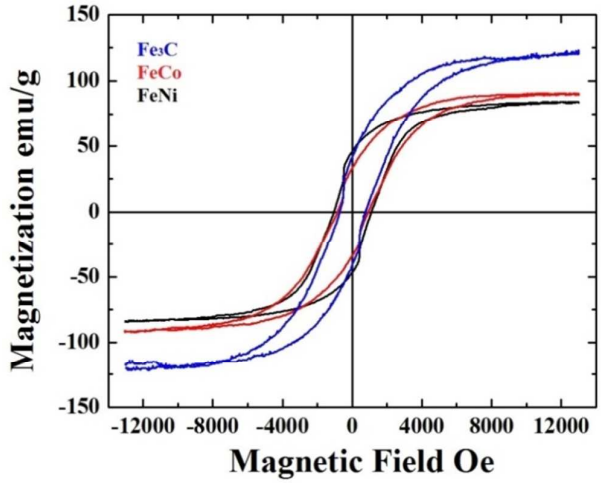

Figure 7: Hysteresis loops measured from buckypapers comprising CNTs filled with continuous Fe_3C (blue hysteresis), FeCo (red hysteresis) and FeNi (black hysteresis) crystals.

Interestingly an extremely high saturation magnetization of 117 emu/g was measured in the case of the buckypaper produced with 30 mg of ferrocene, while slightly lower saturation magnetizations are obtained in the case of FeCo (90 emu/g) and FeNi (80 emu/g). The measured coercivity was 790 Oe in the case of the first buckypaper (CNTs filled with Fe_3C), 858 Oe in the case of FeCo and 1066 Oe in the case of FeNi. The measured saturation magnetizations are much higher with respect to those previously measured in literature in the case of continuous Fe_3C crystals inside CNTs [18,19,21] and in the case of small Fe_3C crystals inside CNTs [8,13].
Furthermore the measured saturation magnetizations are also much higher with respect to those measured in the case of FeCo, FeNi and CoFeNi alloys reported in previous literature reports [23-30].
However the magnetic properties measured in the case of the FeNi sample are much lower with respect to those of 140 emu/g and of 160 emu/g measured in the case of FeNi nanoparticles reported by Kurlyandskaya[30] et al. (produced through electric explosion of wire) and Ghisari et al. (prepared by ball milling)[31].
This difference could be associated to local crystallite arrangements. Indeed analyses of the XRD patterns (see Fig.S3) revealed a grain size in the order of 30 nm, suggesting that the encapsulated FeNi alloy may possess a multigrain arrangement[2].
Furthermore, the lower saturation magnetization may be associated also to a variable filling rate of the CNTs.
Unusual step-like features are also observed in the measured hysteresis loops. The origin of these features is beyond the scope of this paper, but could be associated to magnetization reversal phenomena of the encapsulated crystals. Interestingly Lv et al. also observed unusual step-like features in the case of CNTs completely filled with Fe_3C crystals[21]. As a last step, being interested in investigating also the magnetic properties of buckypapers comprising CNTs filled with Co, Ni and CoNi, further experiments were performed with cobaltocene (30 mg), nickelocene (30 mg) and nickelocene (15 mg) and cobaltocene (15 mg). Indeed, to the best of our knowledge, no buckypapers comprising CNTs filled with Co, Ni and CoNi have been previously reported. Interestingly, as a result, buckypapers with different morphology were obtained. As shown in Fig. 8-9 the SEM investigations of the buckypapers obtained from CVD of nickelocene and cobaltocene-nickelocene and peeled-off from the Si/SiO_2 substrate revealed the presence of CNTs partially-filled with small particles. The typical morphology of the obtained buckypaper can be observed in Fig.8A from a top view. In Figs.8B-D the cross section of the buckypaper shows that in this case a smaller buckypaper-thickness of 5-7 micrometres is present. In particular the XRD measurements of the buckypaper comprising CoNi revealed the presence of the CoNi 1:1 cubic structure (see FigS4) with grain size of 25.6 nm.
The CNTs morphology is shown in higher detail in Fig.8C and 9A,C. In particular the encapsulated particles (diameter of 100-150 of nm verified with high resolution BE imaging in Fig.9B) were observed in Figs.8D and 9B and analysed through EDX as shown in Fig.9D. Differently the morphology of the buckypapers obtained in the case of the CVD of the only cobaltocene (Fig.10) revealed the formation of agglomerates (diameter of 30-40 micrometres) of Co nanoparticles (see BE in Fig.10B and EDX in Fig.10D) embedded by amorphous carbon layers (see Fig.10A-C). Indeed the XRD analyses performed in this latter case did not reveal any reflection corresponding to the 002 plane of the graphitic CNTs-walls.

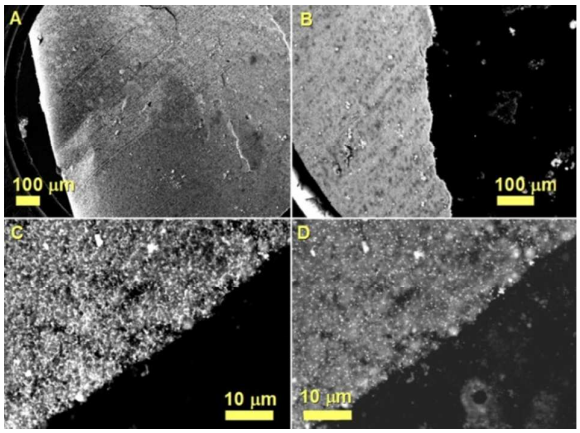

Figure 8: SEM micrographs showing in A-C the surface-morphology and in D the atomic-contrast (CNTs-filling rate) of the buckypaper comprising CNTs-partially filled with CoNi. Similar buckypaper was also obtained in the case of CVD of the only nickelocene (buckypaper-CNTs filled with low quantities of small Ni particles).

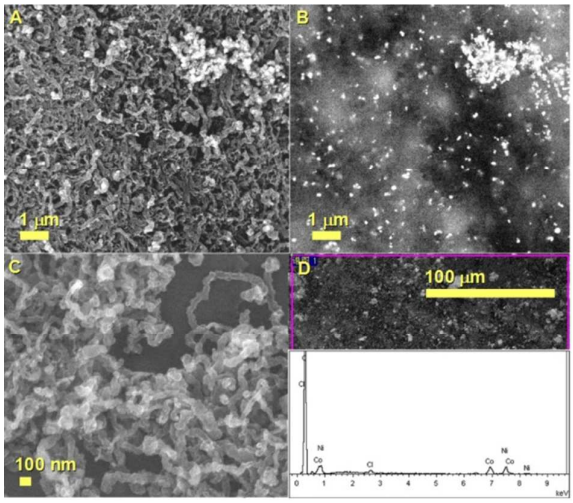

Figure 9: SEM micrographs showing in A-C a higher detail of the surface-morphology and filling rate (BE in B) of the buckypaper comprising CNTs partially filled with CoNi particles. In D the elemental analyses of the area selected with the magenta square shows the presence of Co and Ni elements in a similar weight % (5.5 weight % for Co and 6 weight % for Ni). Similar results were obtained for single particles analyses.

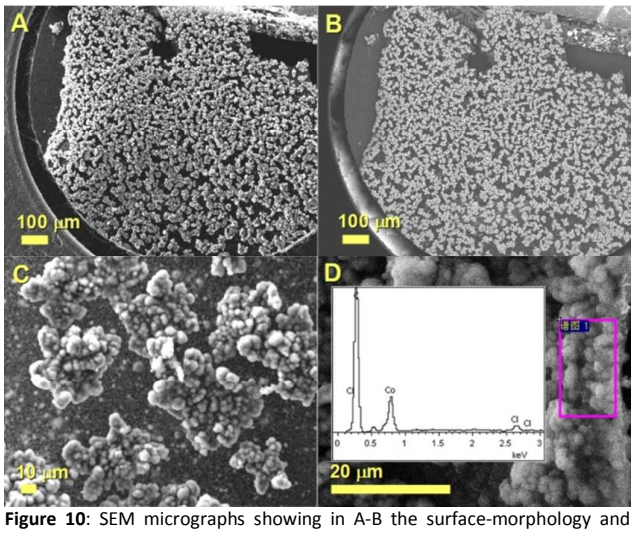

Figure 10: SEM micrographs showing in A-B the surface-morphology and atomic contrast (B) of the buckypaper comprising agglomerates of Co particles embedded in amorphous carbon. In C an higher detail is shown. In D the elemental analyses show the presence of Co up to 20 weight % with carbon (from the amorphous carbon film and from the carbon tape) and Cl (residue from possible HCl droplets in the pyrolyzed cobaltocene/dichlorobenzene vapour).

The magnetic properties of the buckypapers comprising CNTs partially filled with Ni and CoNi and agglomerates of Co nanoparticles (in the case of the CVD of cobaltocene) were then investigated also in this case by VSM. The resulted hysteresis loops are shown in Fig.11. Interestingly lower saturation magnetizations with respect to those measured in the case of the Fe_3C, FeCo and FeNi alloy-filled CNTs-buckypapers were revealed. The measured saturation magnetizations were 70 emu/g for the Co-agglomerates buckypaper, 58 emu/g for the CoNi, partially-filled CNTs-buckypaper and 6.7 emu/g for Ni partially-filled CNTs-buckypaper. The coercivity was found to be 873 Oe for both the cases of Co and CoNi, and 634 Oe for the case of Ni. In particular the low saturation magnetization measured in the case of Ni and CoNi can be associated to the low filling rate of the CNTs comprised in the produced buckypaper and to possible multigrain arrangement[2]. Temperature dependence measurements performed with superconducting quantum interference device at 5K and 150K (see sup. Info. Fig.S-5-6) revealed no remarkable variation of the saturation magnetization. Only small variations of the coercive force are found, probably due to the broken CNTs-alignment during the sample preparation. In particular, to confirm the key role of the continuous filling rate in the control of the saturation magnetization the magnetic properties of the produced buckypapers with FeCo and FeNi were compared with additional CNTs films samples partially filled with FeCo or FeNi particles prepared in simial r conditions but without dichlorobenzene (see Fig.S7-S8 in Sup Info). In this case lower saturation magnetizations of 34/36 emu/g were found for mixed Fe_3C/FeNi (Fm-3m and P1m1) alloys with grain size of 27.3 nm while a saturation magnetization of 65 emu/g was measured for FeCo alloys with grain size of 31.57 nm. The weaker saturation magnetization can be therefore associated also to the lower filling rates of the forest-like CNTs with respect to the filled-CNTs produced with dichlorobenzene. This is in agreement also with recent low-temperature studies performed on CNTs completely filled with α-Fe[18] (produced with perturbed-CVD) where (after subtraction of diamagnetic contribution of CNTs present at low temperature) a saturation magnetization of 189.5 emu/g, much higher with respect to that obtained in the case of partially filled CNTs, was found.

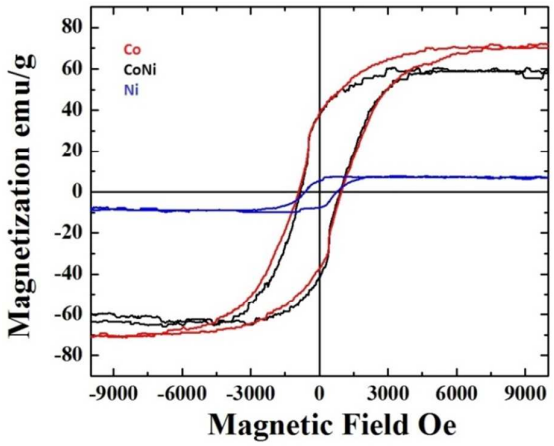

Figure 11: Hysteresis loops measured from buckypapers comprising CNTs filled with small CoNi (black hysteresis) and Ni (blue hysteresis) crystals. The Co agglomerates-buckypaper hysteresis is indicated in red.

Conclusions

In summary we reported an advanced study of synthesis and characterization of cm-length ultrathin buckypapers from CVD of

single metallocene (ferrocene, cobaltocene, nickelocene) or metallocenes combinations (ferrocene-cobaltocene, ferrocene-nickelocene, cobaltocene-nickelocene) with small-fixed quantities of dichlorobenzene (0.05 ml).

After each reaction the as synthesized buckypaper was peeled-off from the Si/SiO_2 substrates and characterized with SEM, BE, EDX, TEM, HRTEM, XRD and VSM. The characterization revealed the presence of continuously filled CNTs (comprised in the buckypaper) only in the case of Fe_3C, FeCo, FeNi alloys obtained by CVD of ferrocene, ferrocene-cobaltocene, ferrocene-nickelocene. Differently in the case of CVD of cobaltocene, cobaltocene-nickelocene and nickelocene buckypapers comprising Co agglomerates embedded in amorphous carbon layers (cobaltocene case) and CNTs partially filled with CoNi and Ni nanoparticles (cobaltocene-nickelocene and nickelocene cases) were found. The magnetic properties investigated with VSM revealed extremely high saturation magnetizations in the case of buckypapers comprising CNTs filled with Fe_3C (117 emu/g), FeCo (90 emu/g), and FeNi (80 emu/g) which are much higher with respect to those reported in literature. Instead the magnetic properties of the buckypapers comprising CNTs partially filled with Ni, CoNi and agglomerates of Co nanoparticles revealed lower saturation magnetizations of 6.7 emu/g, 58 emu/g and 70 emu/g respectively. To the best of our knowledge, no reports have previously shown such high magnetic tunability in thin buckypapers. Furthermore no reports have previously shown buckypapers comprising CNTs filled with Ni, CoNi and Co.

We attribute the remarkable difference with the magnetic properties measured in literature to the very low quantity of dichlorobenzene used in our CVD approach, to the CNTs filling rates and to the crystallite grain-arrangement present in our samples. We also expect that in presence of high quantities of dichlorobenzene or similar hydrocarbons, much higher quantities of Cl would be present inside the CNTs-filling and this may also affect the magnetism of the obtained crystals, since large quantities of Cl would etch the crystal-lattice of the catalyst. The synthesis of these buckypapers could be scaled-up considering a concentration of metallocene of 600 mg/ml and keeping a constant sublimation rate at the temperature reported in the experimental section.

C: Experimental

Synthesis

Mixtures of dichlorobenzene and metallocenes were sublimated and pyrolyzed in a chemical vapour deposition system comprising a quartz-tube reactor of 1.5 m, outer diameter of 22 mm and wall thickness of 2.5 mm, smooth Si/SiO_2 substrates (1 cm length, 1 cm width and 0.5 mm thickness) and an electrical furnace with a temperature of 990 °C [20-22]). The sublimation temperature was 300 °C. The mixture was sublimated in 1 min at the Ar flow rate (laminar flow) of 10 ml/min; the total reaction time was 5-10 minutes. The sample was cooled down by removing the furnace along a rail system. In order to investigate the optimum synthesis conditions, the first reactions were performed with 30 mg and 40 mg of ferrocene each one mixed with a constant quantity of dichlorobenzene of 0.05 ml (1 drop). After definition of the optimum synthesis conditions the introduction of other metallocenes or combinations were considered. The quantities of metallocene used for these reactions were: 1) ferrocene(15mg)-cobaltocene(15mg), 2) ferrocene(15mg)-nickelocene(15mg), 3) cobaltocene (30 mg), 4) cobaltocene(15mg)-nickelocene(15mg) and 5) nickelocene (30 mg).

Structural characterization

The morphological characterization was performed through SEM, BE, and EDX with a JSM-7500F at 5-20 kV. The cross-sectional STEM, TEM and HRTEM analyses were performed with a 200 kV American FEI Tecnai G^2F20. Elemental composition was investigated through EDX performed with STM mode. The magnetic properties were investigated through VSM at room temperature with a VSM 2.5 Tesla electromagnet East Changing 9060 at the magnetic field of 1.3 Tesla and SQUID at 5 K and 150 K.

Acknowledgements

We acknowledge Prof. Gong Min for his continuous support in this research work. We are also grateful for the financial support from the National Natural Science Foundation of China (Grant Nos. 11004141 and 11174212), the Program for New Century Excellent Talents in University of Ministry of Education of China (Grant No. 11-0351), the Project supported by the Scientific Research Staring Foundation for the Returned Overseas Chinese Scholars, Ministry of Education of China and for financial support from National Natural Science Foundation of China (Grant No. 61307039). We also acknowledge the International Cooperation and Exchange of Science and Technology Project in Sichuan Province under Grant No.2013HH0010.

References

1 H. Terrones, F. López-Urías, E. Muñoz-Sandoval, J. A. Rodríguez-Manzo, A. Zamudio, A. L Elías, et al. Solid State Sciences, 2006, **8**, 303.

2 F. S. Boi, S. Maugeri, J. Guo, M. Lan, S. Wang, J. Wen, G. Mountjoy, M. Baxendale, G. Nevill, R. M. Wilson, Y. He, S. Zhang, and G. Xiang Appl. Phys. Lett., 2014, **105**, 243108.

3 A. Leonhardt, M. Ritschel, M.; Elefant, D. N. Mattern, K. Biedermann, S. Hampel, Ch. Muller, T. Gemming, B. Buchner.

Journal of Applied Physics, 98, 074315 (2005).

4 A. L. Danilyuk, A. L. Prudnikava, I. V. Komissarov, K. I. Yanushkevich, A. Derory, F. Le Normand, V. A. Labunov, S. L. Prischepa. Carbon, 2014, **68**, 337.

5 F. C. Dillon, A. Bajpai, A. Koos, S. Downes, Z. Aslam, N. Grobert Carbon, 2012, **50**, 3674.

6 S. Hampel, A. Leonhardt, D. Selbmann, K. Biedermann, D. Elefant, Ch. Muller, T. Gemming and B. Buchner. Carbon, 2006, **44**: 2316.

7 A. Leonhardt, M. Ritschel, R. Kozhuharova, A. Graff, T. Muhl, R. Huhle, I. Monch, D. Elefant and C.M. Schneider. Diamond and Related Materials, 2003, **12**, 790.

8 A. Morelos-Gomez, F. Lopez-Urias, E. Munoz-Sandoval, C. L. Dennis, R. D. Shull, H. Terrones and M. Terrones. Journal of Material Chemistry 2010, **20**, 5906.

9 C. Muller, S. Hampel, D. Elefant, K. Biedermann, A. Leonhardt, M. Ritschel, B. Buchner. Carbon, 2006; **44**, 1746.

10 D. Golberg, M. Mitome, Ch. Muller, C. Tang, A. Leonhardt, Y. Bando. Acta Materialia, 2006, **54**, 2567.

11 C. Prados, P. Crespo, J. M. Gonzalez, A. Hernando, J. F. Marco, R. Gancedo, N. Grobert, M. Terrones, R. M. Walton and H. W. Kroto. Physical Review B, 2002, **65**, 113405.

12 J. F. Marco, J. R. Gancedo, A. Hernando, P. Crespo, C. Prados, J. M. Gonzalez N. Grobert, M. Terrones, D. R. M. Walton and H. W. Kroto. Hyperfine Interactions, 2002, **139**, 535.

13 S. Karmakar, S. M. Sharma, M. D. Mukadam, S. M. Yusuf, A. K. Sood. Journal of Applied Physics, 2005, **97**, 054306.

14 C. Muller, D. Golberg, A. Leonhardt, S. Hampel, B. Buchner. Physica status solidi (a), 2006, **203**, 1064.

15 U. Weissker, S. Hampel, A. Leonhardt, B. Buchner. Materials 2010, **3**, 4387.

16 J. Cheng, X. P. Zou, G. Zhu, M. F. Wang, Y. Su, G. Q. Yang, et al. Solid State Communications 2009, 149, 1619-22.

17 S. Groudeva-Zotova, R. Kozhuharova, D. Elefant, T. Muhl, C. M. Schneider, I. Monch. Journal of Magnetism and Magnetic Materials 2006, **306**, 40–50.

18 F. S. Boi, G. Mountjoy, R. M. Wilson, Z. Luklinska, L. J. Sawiak, M. Baxendale. Carbon 2013, **64**, 351-8.

19 F. S. Boi, G. Mountjoy, M. Baxendale. Carbon, 2013; **64**, 516.

20 W. Wang, K. Wang, R. Lv, W. J. Zhang, X Kang, F. Chang et al. Letters to the Editor Carbon 2007; **45**, 1105-36.

21 R. Lv, S. Tsuge, X. Gui, K. Takai, F. Kang,T. Enoki,, J. Wei, J. Gu, K. Wang, D. Wu Carbon, 2009, **47**, 1141.

22 X. Gui, K.Wang,W. Wang, J. Wei, X. Zhang, R. Lv, Y. Jia, Q.Shu, F. Kang, D. Wu. Materials Chemistry and Physics, 2009, **113**, 634–637.

23 R. Lv, F. Kang, W. Wang, J. G J. Wei, K. Wang, D.Wu. Carbon, 2007, **45**, 1433.

24 R. Lv, A. Cao, F. Kang, W. Wang, J. Wei, J. Gu. J. Phys. Chem. C, 2007, **111**, 11475.

25 R. Lv, F. Kang, J. Gu, X. Gui, J. Wei, K. Wang and D. Wu. Applied Physics Letters, 2008, **93**, 223105.

26 F. S. Boi, G. Mountjoy, Z. Luklinska, L. Spillane, L. S. Karlsson, R. M. Wilson, A. Corrias, M. Baxendale. Microscopy and Microanalysis 2013, **19**, 1298.

27 N. Grobert, M. Mayne, M. Terrones, J. Sloan, R. E. Dunin-Borkowski, R. Kamalakaran, T. Seeger, H. Terrones, M. Ruhle, D. R. M. Walton, H. W. Kroto and J. L. Hutchison. Chem. Commun., 2001, 471–2.

28 A.L. Elıas, J. A. Rodrıguez-Manzo, M. R. McCartney, D. Golberg, A. Zamudio, S. E. Baltazar, F. Lopez-Urıas, E. Munoz-Sandoval, L. Gu, C. C. Tang, D. J. Smith.; Y. Bando, H. Terrones, M. Terrones. Nano Lett., 2005, **5**, 467.

29 D. Hisada, Y. Fujiwara, H. Sato, M. Jimbo, T. Kobayashi, K. Hata. Journal of Magnetism and Magnetic Materials, 2011, **323**, 3184.

30 M. Y. Rafique, L. Pan, M. Z. Iqbal, Q. Javed, H. Qiu, R. Ud-din, M.H. Farooq, Z. Guo. Journal of Alloys and Compounds, 2013, **550**, 423.

30 G.V. Kurlyandskaya , I. Madinabeitia , I.V. Beketov, A.I. Medvedev, A. Larranaga , A.P. Safronov , S.M. Bhagat. Journal of Alloys and Compounds, 2014, **615**, S231.

31 J.T. Oh Ghisari, S. Javapour, J. Magn. Magn. Mater., 2011, **1020**, 509